Final Draft
of the original manuscript:

Novel approach for the treatment of cyclic loading using a potential-based cohesive zone model

Ingo Scheider*, Jörn Mosler

Helmholtz-Zentrum Geesthacht, Max-Planck-St. 1, D-21502 Geesthacht, Germany

Abstract

The development of cohesive zone models in the finite element framework dates back some 30 years, and cohesive interface elements are nowadays employed as a standard tool in scientific and engineering communities. They have been successfully applied to a broad variety of different materials and loading scenarios. However, many of such constitutive models are simply based on traction-separation relations without deducing them from energy potentials. By way of contrast, a thermodynamically consistent cohesive zone model suitable for the analysis of low cycle fatigue is elaborated in the present contribution. For that purpose, a plasticity-based cohesive law including isotropic hardening/softening is supplemented by a damage model. First results of this new approach to cyclic loading will be presented illustrating the applicability to low cycle fatigue.

Cohesive interfaces; Damage mechanics; Low cycle fatigue, Fracture;

1. Introduction

Cohesive zone models for material separation and eventually failure of solids have been introduced within the finite element framework by Hillerborg [1] in 1977 for the first time. Since 1992 they have been used for fracture of ductile materials, cf. [2]. While cohesive zone models have exclusively been applied to monotonous loading until 1999, several groups have also subsequently introduced cohesive zone models for fatigue crack growth, see [3] and [4].

Nomenclature	
d	damage variable (d=0: undamaged, d=1: fully damaged)
Q^i	stress-like plasticity variable
$[\![\mathbf{u}]\!]$	displacement jump
$\mathbf{T}$	traction vector
Y	energy release rate
α^i	displacement-like plasticity variable (isotropic hardening)

----

* Corresponding author. Tel.: +49-4152-872599; fax: +49-4152-8742599.
E-mail address: ingo.scheider@hzg.de.

| $\dot{\lambda}$ | plastic multiplier |
| ψ | Helmholtz energy |

Many constitutive laws for cohesive interfaces under monotonous loading are not based on potentials (Helmholtz energy) and hence, they have never been proven to be in accordance with thermodynamical principles, cf. e.g. [5]. The traction-separation law shown in Fig. 1 is the one-dimensional representation of the model presented in [5]. It has been shown in various examples that for engineering structures the model leads to reasonable results, but a unique formulation for loading/unloading, tension/compression, which also complies with the restrictions imposed by the second law of thermodynamics, is still missing. Such a unique formulation will be presented here. This newly derived model opens up the possibility of using a unified framework for monotonous and cyclic loading. A similar model has also been proposed by Grassl for concrete [6].
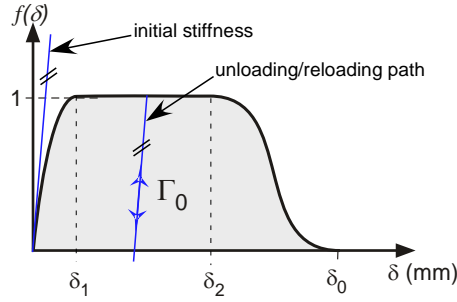

Fig. 1: Traction-separation law defined in [5].

In the following, a new interface model including damage accumulation and plasticity will be developed that is suitable for the modeling of fracture and failure of real structures under monotonous and cyclic loading conditions. The model is derived from the Helmholtz energy and splits the material separation in elastic and plastic parts. It uses an internal variable for isotropic hardening as well as another variable for material degradation. The present paper will expose the theory of the general capabilities comparing the predicted failure behavior with analytical, but purely heuristic approaches for low cycle fatigue (Coffin-Manson rule).

2. Fundamentals

The geometry of a cohesive element is defined by two facets with their coordinates $\mathbf{X}^+$ and $\mathbf{X}^-$ in the reference configuration and $\mathbf{x}^{\pm} = \mathbf{X}^{\pm} + \mathbf{u}^{\pm}$ in the current configuration, respectively. The displacement jump writes $[\![\mathbf{u}]\!] = \mathbf{u}^+ - \mathbf{u}^-$ and can be split additively into a reversible part (in the following called *elastic*) and an irreversible part (accordingly, called *plastic*), i.e.

$$[\![\mathbf{u}]\!] = [\![\mathbf{u}]\!]^{el} + [\![\mathbf{u}]\!]^{pl} \tag{1}$$

The constitutive behavior of the interface model is based on a Helmholtz energy of the form

$$\rho\psi([\![\mathbf{u}]\!], \alpha^i, d) = (1-d)(\tfrac{1}{2}c\,[\![\mathbf{u}]\!]^{el} \cdot [\![\mathbf{u}]\!]^{el}) + \rho\psi^i(\alpha^i) \tag{2}$$

which is in accordance with continuum plasticity and damage mechanics. The quantity α^i denotes an internal variable for isotropic hardening, d is a damage variable. Equation (2) describes a general interface behavior, from which the stress-like conjugate variables, namely the stress vector, **T,** acting on the interface, the internal variable Q^i associated with isotropic hardening (conjugate to α^i) and the energy release rate Y are calculated by computing the derivative of eq. (2) with respect to the work conjugate variables. Following the effective stress concept (strain equivalence), the energy related to a fictitious undamaged state is introduced by

$$\rho\tilde{\psi}(\llbracket\tilde{\mathbf{u}}\rrbracket, \tilde{\alpha}^i) = \tfrac{1}{2}c\llbracket\tilde{\mathbf{u}}\rrbracket^{el} \cdot \llbracket\tilde{\mathbf{u}}\rrbracket^{el} + \psi^i(\tilde{\alpha}^i) \tag{3}$$

and the displacement-like variables fulfill the identities $\llbracket\tilde{\mathbf{u}}\rrbracket = \llbracket\mathbf{u}\rrbracket$, $\llbracket\tilde{\mathbf{u}}\rrbracket^{pl} = \llbracket\mathbf{u}\rrbracket^{pl}$ and $\tilde{\alpha}^i = \alpha^i$. With such assumptions, the stress-like variables can be defined as

$$\begin{aligned} \mathbf{T} &= \rho\partial_{\llbracket\mathbf{u}\rrbracket}\psi = (1-d)c\,\llbracket\mathbf{u}\rrbracket^{el} & \tilde{\mathbf{T}} &= \partial_{\llbracket\tilde{\mathbf{u}}\rrbracket}\tilde{\psi} = \frac{\mathbf{T}}{(1-d)} \\ Q^i &= -\rho\partial_{\alpha^i}\psi^i & \tilde{Q}^i &= -\rho\partial_{\alpha^i}\tilde{\psi}^i = Q^i \\ Y &= \rho\partial_d\psi = -\tfrac{1}{2}c\,\llbracket\mathbf{u}\rrbracket^{el} \cdot \llbracket\mathbf{u}\rrbracket^{el} \end{aligned} \tag{4}$$

In line with standard (continuum) plasticity theory, the elastic domain is defined by a yield function f ($f<0$ spans the elastic regime) and the evolution equations are derived from a plastic potential g. Both functions are expressed in terms of effective stress quantities. More specifically,

$$\begin{aligned} f(\tilde{\mathbf{T}}, \tilde{Q}^i) &= \tilde{T}^{eq}(\tilde{\mathbf{T}}) - (\tilde{Q}_0^i + \tilde{Q}^i) \\ g(\tilde{\mathbf{T}}, \tilde{Q}^i, Y) &= f(\tilde{\mathbf{T}}, \tilde{Q}^i) - \frac{SY}{(1-d)} \end{aligned} \tag{5}$$

Here, S is a material parameter driving the damage accumulation and $\tilde{Q}_0^i$ defines an initial yield stress. For capturing a different strength in normal and tangential separation, the effective stress $\tilde{T}^{eq}$ is decomposed into its normal T_n and tangential $\mathbf{T_t}$ components. With this split, the equivalent stress defining the shape of the yield function is assumed to be of the type $T^{eq} = \sqrt{(T_n)^2 + \beta(\mathbf{T}_t)^2}$ with β being an additional material parameter. The model is completed by suitable evolution equations. Computing the derivatives of the convex plastic potential, they are postulated to be of the type

$$\begin{aligned} \llbracket\dot{\mathbf{u}}\rrbracket^{pl} &= \dot{\lambda}\,\partial_{\mathbf{T}}g = \frac{\dot{\lambda}}{(1-d)}\partial_{\tilde{\mathbf{T}}}g \\ \dot{\alpha}^i &= -\dot{\lambda}\,\partial_{Q^i}g = \dot{\lambda} \\ \dot{d} &= -\dot{\lambda}\,\partial_Y g = \frac{\dot{\lambda}}{(1-d)}\,S(-Y)^{M-1} \end{aligned} \tag{6}$$

Collecting all equations, the final model requires a set of five parameters for the three-dimensional case (if linear isotropic hardening is assumed): c, β, Q_0^i, H^i, S.

In the following section, the capabilities of the model for different loading situations will be shown.

3. Application

3.1. Parameter selection

The model is applied to a prescribed normal displacement jump, while the tangential part remains zero (i.e. the parameter β does not have any effect on the results in this case). For plasticity, a nonlinear isotropic hardening function with saturation stress of the form

$$Q^i(\alpha^i) = Q_\infty(1 - \exp(-b\alpha^i)) \qquad (7)$$

with two parameters, Q_∞, b, is employed. The material parameters used throughout the investigation are given in Table 1.

Table 1: Cohesive zone model parameters used for the simulations

c [N/mm^3]	Q_0^i [MPa]	b [mm^{-1}]	Q_∞ [MPa]	S
1,000,000	100.0	200.0	100.	1.0

One may argue that the elastic deformation of a cohesive interface without any material volume should be negligible. Therefore, the stiffness, c, is chosen as very stiff. More precisely, the separation at which plasticity occurs is only 10^{-4} mm. Already after a plastic separation of only 0.02 mm, 99% of the saturation stress is reached. A simple analytical approximation of the maximum separation at which failure occurs, can be given for the assumption $[\![\mathbf{u}]\!]^{el} \to 0$. For pure normal separation, $[\![\mathbf{u}]\!] \approx \frac{\lambda}{(1-d)}$ holds. Thus, inserting this into eq. (6).3 leads to a linear relation between damage and separation ($d \approx [\![\mathbf{u}]\!] S$). Consequently, the separation at final failure can eventually be approximated in this case by

$$[\![\mathbf{u}]\!]_{(d=1)} \approx \tfrac{1}{S}. \qquad (8)$$

3.2. Monotonous loading

The first load case under consideration is monotonous, which leads to a critical separation of $[\![\mathbf{u}]\!]_{(d=1)} \approx 1$ for the parameters given in Table 1 (see eq. (8)). The stress acting on the interface and the internal plastic variable, α, are shown in Fig. 2. The small number of parameters indeed limits the possibility of shaping the traction-separation law. However, the physical parameters, maximum cohesive strength and critical separation can be identified by specifying the model parameters, Q_∞, S, accordingly.
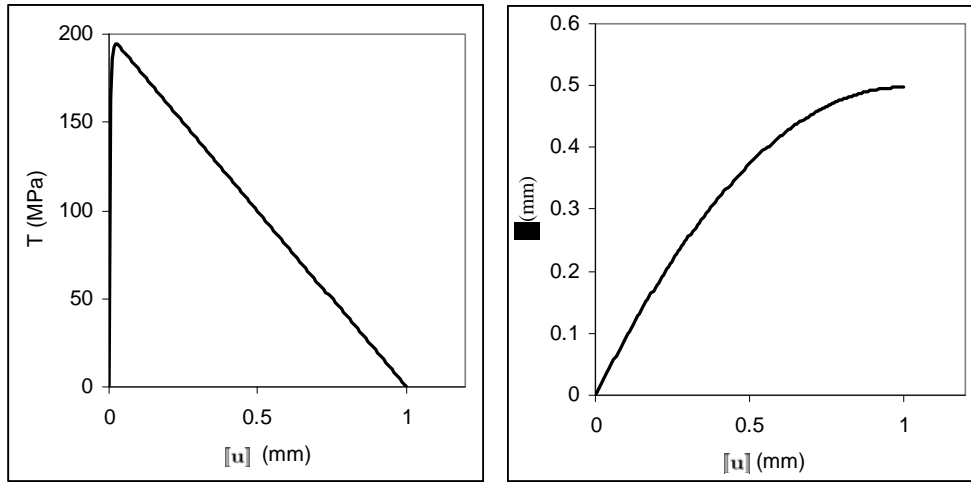
Fig. 2: Mechanical response predicted by the model for a monotonous normal separation: stress acting on interface (left) and internal variable associated with plastic deformation (right)

3.3. Cyclic loading

If the maximum separation is smaller than the critical value, the material point can still fail due to damage accumulation, if it is loaded cyclically. In the present example, the loading is a swelling separation between maximum value of $[\![\mathbf{u}]\!]_{max} = 0.1$ mm and $[\![\mathbf{u}]\!]_{min} = 0.0$ mm. In Fig. 3 (left), the resulting stresses at the interface are shown. While the equivalent stress (solid black line) is constant under compressive loading, the normal stress exhibits plasticity acting both in tension and compression. The damage in the right graph of Fig. 3 (red line) shows that degradation only occurs under tensile loading (damage is constant otherwise), while plastic separation occurs in both loading directions.
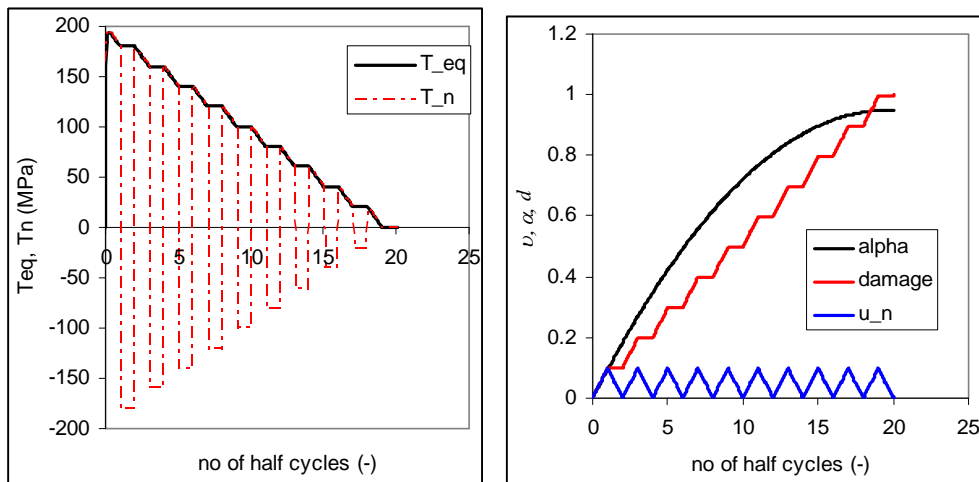

Fig. 3: Results for cyclic loading with $[\![\mathbf{u}]\!]_{max} = 0.1$ mm. Left: The equivalent and the normal stress; Right: Evolution of damage and internal variable associated with plasticity

A further study aims at investigating the effect of straining on the number of cycles to failure. The major resource for a comparison is the Coffin-Manson rule, which postulates a power law relation between the amplitude of the plastic strain increment and the number of cycles, i.e. a straight line in a log-log plot.

For this study, several loading amplitudes are considered with a maximum separation between 0.0025 and 0.25. The computed graph is given in Fig. 4. Accordingly, a good agreement between the model simulations and the Coffin-Manson rule can be seen.
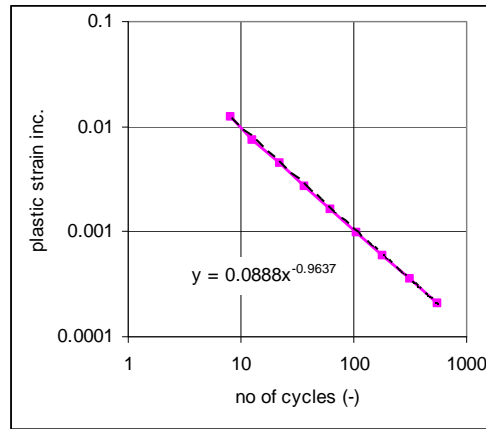

Fig. 4: Low cycle fatigue behavior simulated by the proposed cohesive zone model. The curve shows a linear relationship between plastic strain increment and the number of cycles to failure in a log-log plot. This is in line with the Coffin-Manson rule.

4. Conclusion

A potential-based cohesive model capable of simulating monotonous and cyclic loading has been presented. The underlying theory contains all ingredients necessary for the modeling of various load cases including different damage evolutions in normal and shear direction. Although the resulting model shows a broad variety of possible applications, it requires only a small number of material parameters. However, extensions (e.g. kinematic hardening, modified equivalent stress or better damage evolution) leading to more flexibility regarding e.g. the shape of the traction-separation law under monotonous loading or more variability in the low-cycle fatigue regime, are easy to implement.

References

[1] Hillerborg A, Modeér M. Petersson PE. Analysis of crack formation and crack growth in concrete by means of fracture mechanics and finite elements. *Cement. Concrete Res* 1976;**6**:773-82.
[2] Tvergaard V, Hutchinson JW. The relation between crack growth resistance and fracture process parameters in elastic-plastic solids. *J. Mech. Phys. Solids* 1992;**40**:1377-97.
[3] deAndrés A, Pérez JL, Ortiz M. Elastoplastic finite element analysis of three-dimensional fatiguew crack growth in aluminium shafts subjected to axial loading. *Int. J. Solids Struct.* 1999;**36**:2231-58.
[4] Yang B, Mall S, Ravi-Chandar K. A cohesive zone model for fatigue crack growth in quasibrittle materials. *Int. J. Solids Struct.* 2001;**38**:3927-44.
[5] Scheider I, Brocks W. Simulation of cup-cone fracture using the cohesive model, *Eng Fract Mech* 2003;**70**:1943-62.
[6] Grassl P, Rempling R. A damage-plasticity interface approach to the meso-scale modelling of concrete subjected to cyclic compressive loading. *Eng Fract Mech* 2008;**75**:4804-18.